

## **Comparison of Different SPECT Images Analysis Methods for Inter-hemispheric Asymmetry Detection in Patients with Epileptic Symptoms**

**ELŻBIETA OLEJARCZYK<sup>1,\*</sup>, MAŁGORZATA PRZYTULSKA<sup>1</sup>,  
ADAM BAJERA<sup>2</sup>, LESZEK KRÓLICKI<sup>2</sup>**

<sup>1</sup> *Institute of Biocybernetics and Biomedical Engineering, Polish Academy of Sciences,  
Warsaw, Poland*

<sup>2</sup> *Medical University of Warsaw, Department of Nuclear Medicine, Warsaw, Poland*

The aim of this work was examination of asymmetries in activity of the left and right cerebral hemispheres as well as localization and contouring of the regions of reduced or increased activity on the basis of single photon emission computed tomography (SPECT) images. The mean and standard deviation of normalized intensities inside the contoured areas of images, entropy based on intensity histograms and Chen's fractal dimension were calculated.

**Key words:** SPECT, epilepsy, fractal dimension, entropy

### **1. Introduction**

The development of a number of applications for brain single photon emission computed tomography (SPECT) as a diagnostic modality and research tool in neurology is observed [1]. Interictal brain SPECT is useful for detection of seizure focus [2, 3]. The use of quantitative methods can improve performance in detection of perfusion asymmetry over visual inspection alone [2, 4, 5, 6].

The aim of this work was examination of asymmetries in activity of the left and right cerebral hemispheres as well as localization and contouring of the regions of reduced or increased activity on the basis of SPECT images [7]. Advantage of this technique is possibility of brain activity map acquisition at the time of radiotracer

---

\* Correspondence to: Elżbieta Olejarczyk, Institute of Biocybernetics and Biomedical Engineering, Polish Academy of Sciences, ul. Ks. Trojdena 4, 02-109 Warsaw, Poland, e-mail: eolejarczyk@ibib.waw.pl  
*Received 21 February 2008; Accepted 04 June 2008*

injection during seizures though the image registration is done one hour after seizure. The SPECT imaging method allows better spatial localization of seizure source than the analysis of EEG signal. Simultaneous EEG signal registration allows to qualify exactly the moment of seizure onset when radiotracer injection could be done to register an unequivocal image. The mean and standard deviation of normalized intensities inside the contoured areas of images were calculated. Methods like entropy based on intensity histograms and Chen's fractal dimension were also applied.

## 2. Materials

The scintigraphic examinations of cerebral perfusion in 6 patients with epilepsy were performed in the Department of Nuclear Medicine of the Medical Academy of Warsaw. The intravenous delivery of the  $Tc^{99m}$  HMPAO with activity about 200 MBq was performed to each patient in interictal phase. The registration, lasting 25 minutes, was started about 30 minutes after the radiotracer injection. The aim of this research was detection of reduction or increasing of perfusion in different brain regions, what (in both cases) could correspond to seizure focus existence in these regions.

The aim of this study was evaluation of differences in radioisotope accumulation levels with respect to the standards. The standards assume that the radio-pharmaceutical agent is equally accumulated in both symmetrically located cerebral structures on any lesion level.

Several transverse cerebral images have been acquired from each patient. The images in the below-shown series have been ordered from the basis to the top of the examined brain; left side of an image corresponds to the right side of the brain and *vice versa*.

**Table 1.** Kind of perfusion and localization of the brain region by medical assessment

Patient id (slices number)	Kind of perfusion	Brain region
1 (15)	Disabled	Left temporal lobe
2 (11)	Increased	Right temporal lobe (numerous movement artifacts)
3 (14)	Disabled	Right frontal temporal lobe
4 (16)	Reduced	Left frontal lobe
5 (15)	Reduced	Left temporal lobe
6 (15)	Disabled	Right frontal temporal lobe

An increased/reduced cerebral perfusion corresponds to a higher/lower isotope density and is manifested by an increased/reduced image luminance registered in an 8-bits scale and normalized to the maximum (256 steps) luminance level respectively. Images of 128x128 pixel size were registered. In Table 1 several examples of medical description of the corresponding cases are given.

Increased perfusion above means that in one of two symmetrical half-structures radioisotope accumulation level is higher, while reduced perfusion means that it is lower than following from the standard. Disabled perfusion means its lower level with respect to the standard.

### 3. Methods

In order to evaluate the effectiveness of various methods, the comparative analyses of the images of the left and right cerebral hemispheres were performed using three independent methods:

- 1) comparison of the mean and standard deviation values,
- 2) comparison of the estimated entropies,
- 3) comparison of the fractal dimensions.

#### 3.1. The Mean and Standard Deviation of Normalized Intensities

The images were processed and analyzed using standard Image Pro Plus (Media Cybernetics) and Microsoft Excel software packages [8]. Each image was geometrically divided into the left and right parts (Fig. 1). For a direct visual assessment of monochromatic images they also were visualized in pseudo colors (maps of pixels intensity). Then the left and right cerebral hemispheres were automatically contoured and the mean and standard deviation of normalized intensity inside the contoured areas of images were calculated (Fig. 2). At the next step the surrounding background, outside the mask selecting the object of interest, from the images was reduced to the 0 level.

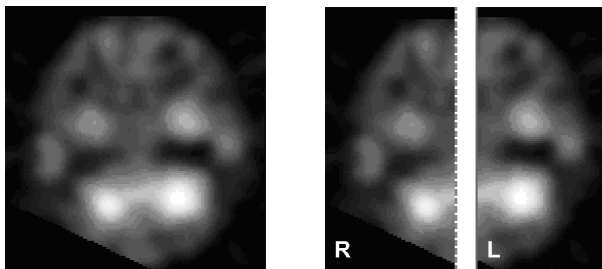
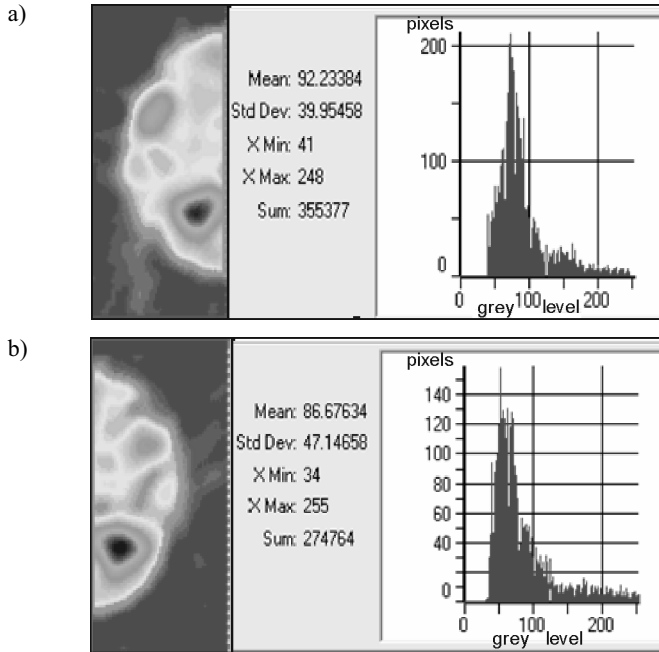


Fig. 1. Image division into the left (L) and right (R) hemispheres for patient 4 slice number 1



**Fig. 2.** Calculation of the mean and standard deviation of intensity in the contours of the left a) and right b) cerebral hemispheres. There are shown examples of images, measured parameters and histograms of intensity for patient 1, slice 1

### 3.2. Entropy Based on Intensity Histograms

The Shannon's entropy [9] of a probability distribution of image intensities is defined as:

$$S = -\sum_{i=1}^N p_i \cdot \log p_i, \quad \sum_{i=1}^N p_i = 1 \quad (1)$$

where  $p_i, i=1, \dots, N$  – probability of  $i$ -th intensity level.

Entropy based on intensity histogram [10] can be estimated as:

$$p_i = \frac{g_i}{g_{total}} \quad (2)$$

where  $g_i$  – number of pixels with intensity  $i$ ;

$g_{total}$  – total number of pixels;

$N$  – number of image gray levels.

Entropy is a measure of information. The bigger are changes of pixel intensities the bigger is the entropy. In this method only total histograms are used to calculate entropy therefore the spatial information is lost.

### 3.3. Chen's Fractal Dimension

For image matrices with dimension  $N \times N$  a multi-scale vector of difference intensity  $MSID = [ri(s1), ri(s2), \dots, ri(sk)]$ , where  $ri(sk)$  – mean intensity of all pairs of pixels at the distance  $sk$ , was defined [11,12].

If  $I(x,y)$  is a measure of intensity (gray level at point with  $(x,y)$  coordinates), then:

$$ri(sk) = \frac{\sum_{x1=0}^{N-1} \sum_{y1=0}^{N-1} \sum_{x2=0}^{N-1} \sum_{y2=0}^{N-1} |I(x2, y2) - I(x1, y1)|}{N_{sk}} \quad (3)$$

$N_{sk}$  – number of pixel pairs for  $sk$  scale

There are the following relations for coordinates  $x1, y1, x2, y2$ :

$$sk = \sqrt{(x2 - x1)^2 + (y2 - y1)^2} \quad (4)$$

$$|\Delta I| = |I(x2, y2) - I(x1, y1)| \propto |\Delta x|^H \quad (5)$$

where:  $H$  – Hurst's exponent (fractal dimension  $Df = 3-H$ );

$\Delta x$  – the distance between points with coordinates  $(x2, y2)$  and  $(x1, y1)$

The logarithms of both sides were calculated:

$$\log |\Delta I| \propto H \cdot \log |\Delta x| \quad (6)$$

## 4. Results

### 4.1. Mean Value and Standard Deviation

The comparative analysis was performed for 6 patients for which mean values and standard deviations of intensity on the left and right cerebral hemispheres were measured. In order to make the results independent on the mean brightness level, data were normalized by calculation of the ratio of the difference to the sum of mean brightness in the hemispheres. The regions of reduced/increased perfusion were located using the above-described image segmentation method. The results of calculations for one patient is shown in Fig. 3. The horizontal axes indicate the numbers of consecutive slices.

### 4.2. Entropy and Fractal Dimension

Entropy and Chen's fractal dimension were calculated for all quarters of brain (upper-left, upper-right, down-left, down-right) in 8 ranges of pixel intensity: 1–32, 33–64, 65–96, 97–128, 129–160, 161–192, 193–224, 225–256. Each of the four regions of brain contains  $63 \times 63$  pixels.

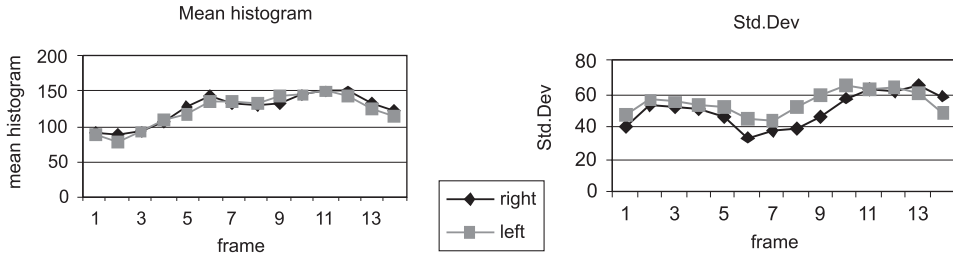


**Fig. 3.** Mean values and standard deviations of intensity for the left and right cerebral hemispheres, patient 1

The ratio of the difference to the sum of entropy and Chen's fractal dimension for left upper/down respect of right upper/down quarter of brain was calculated. Entropy results confirmed the medical observations (Table 2).

**Table 2.** Slices numbers for which the rate of the difference to the sum of S or Df in the left and right hemispheres in range with the biggest intensity of pixels (from 193 to 256) has values bigger than 0.1 for four regions of brain (UL-upper left, UR-upper right, DL-down left, DR-down right)

Patient id	Number of slices for entropy UL-UR-DL-DR	Slices number for fractal dimension UL-UR-DL-DR
1	3-7-8-0	6-1-1-3
2	1-7-4-2	1-1-0-0
3	10-0-9-0	0-0-0-0
4	1-7-7-0	1-1-0-4
5	0-9-3-5	1-0-0-0
6	3-3-2-0	1-0-0-5

A map of pixels intensity for patient 1 is shown in Fig. 4 (slices 7, 8, 9). The bigger fractal dimension in right down part of image for slices 7, 8, 9 was found. In this region clear increased activity is visible on the image.

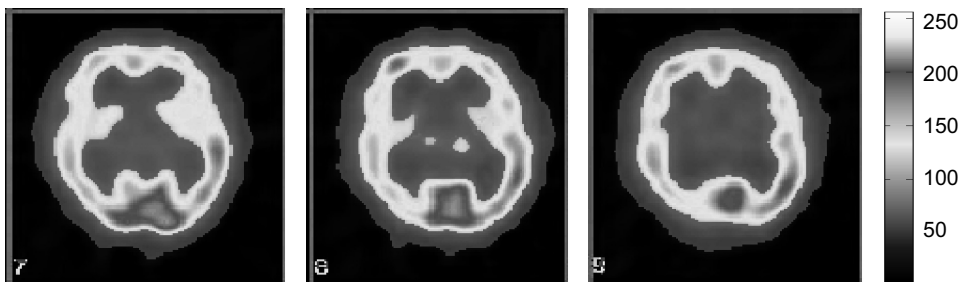


**Fig. 4.** Maps of pixels intensity for patient 1 (slice 7, 8, 9). Grayscale representation corresponds to the resolution of measured intensity (256 levels of pixels intensity)

Graphs of entropy and Chen’s fractal dimension for the higher level of pixel intensity (225–256) in regions of brain where the differences of these measures between both hemispheres are bigger than 10% are shown in Fig. 5.

Histograms of entropy and fractal dimension (Fig.6) show significant differences for the higher level of pixel intensity.

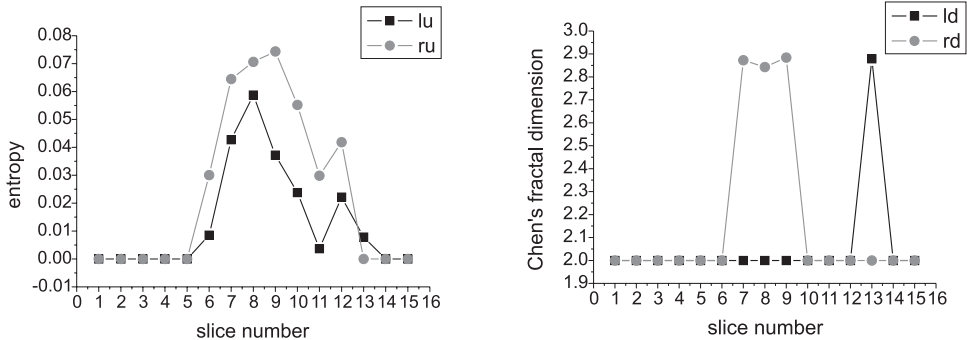


**Fig. 5.** Entropy and Chen’s fractal dimension graphs for the higher level of pixels intensity (225–256) for patient 1 in regions of brain where differences of these measures between both hemispheres are bigger than 10%. Abbreviations meaning is for lu: left-up, ru: right-up, ld: left-down, rd: right-down

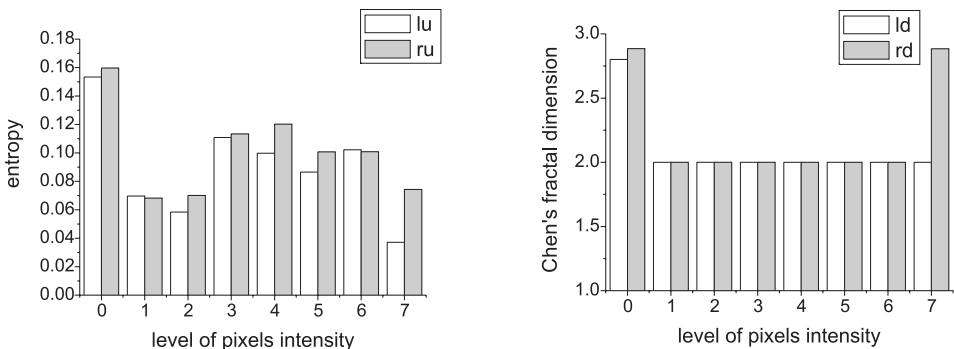


**Fig. 6.** Histogram of entropy and Chen’s fractal dimension for all levels of pixels intensity for patient 1 in regions of brain where differences of these measures between both hemispheres are bigger than 10%. Abbreviations meaning is for lu: left-up, ru: right-up, ld: left-down, rd: right-down

**4.3. Comparison of Three Methods**

Three independent methods: mean luminance, entropy and Chen’s fractal dimension, were compared. The ratio of differences to sum between left and right hemisphere was calculated for every measure (Fig. 7).

It may be seen that entropy is the most sensitive measure. The bigger changes have been seen for upper slices corresponding to frontal lobe localization. The mean

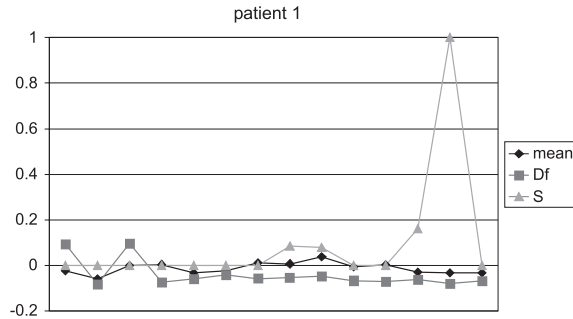


**Fig. 7.** Comparison of three methods: mean luminance, entropy (S) and Chen's fractal dimension (Df) for patient 1

luminance and Chen's fractal dimension had lower but comparable sensitivity. These measures had opposite sign.

## 5. Conclusions

The above-presented methods of cerebral SPECT images analysis based on simple image processing methods and calculation of basic statistical parameters are effective tools for a preliminary assessment of cerebral perfusion changes in patients with epilepsy or cerebral ischemic patients.

It was found that for reduced perfusion entropy increases and Chen's fractal dimension decreases. Entropy based on the intensity histograms permits to evaluate automatically perfusion asymmetry between left and right brain hemisphere taking into account only the bigger intensities of pixels (in the range from 193 to 256). Entropy is a better measure to estimate the global intensity, however – without information about spatial distribution. For identification of epileptic seizure localization (concentration of high intensity pixels) Chen's fractal dimension seems to be the better measure.

In further work calculations for more patients and group of healthy volunteers should be done. Chen's fractal dimension could be calculated for less-dimensional matrices (8 x 8) in sliding window to construct map of fractal dimension of the whole brain. It will allow to estimate better the usability of this method to locate the epileptic seizure and compare different regions of interest (ROIs).

Further extension could be done for investigating the application of fractal dimension based on the intensity histograms to compare different regions of interest [13].

## Acknowledgment

This work was partially supported by Ministry of Science and Higher Education of Poland, project nr 4211/BT02/2007/33.



## References

1. Warwick J.M.: Imaging of brain function using SPECT. *Metab. Brain. Dis.* 2004 Jun, 19(1–2), 113–123.
2. Aubert-Broche B., Jannin P., Biraben A., Bernard A.M., Haegelen C., Le Jeune F.P., Gibaud B.: Evaluation of methods to detect interhemispheric asymmetry on cerebral perfusion SPECT: application to epilepsy. *J. Nucl. Med.* 2005 Apr, 46(4), 707–713.
3. Takano A., Shiga T., Kobayashi J., Adachi I., Nakamura F., Koyama T., Katoh C., Morita K., Tsukamoto E., Tamaki N.: Thalamic asymmetry on interictal SPECT in patients with frontal lobe epilepsy. *Nucl. Med. Commun.* 2001 Mar, 22(3), 319–324.
4. Aubert-Broche B., Grova C., Jannin P., Buvat I., Benali H., Gibaud B.: Detection of inter-hemispheric asymmetries of brain perfusion in SPECT. *Phys. Med. Biol.* 2003 Jun 7, 48(11), 1505–1517.
5. Kovalev V.A., Thurffjell L., Lundqvist R., Pagani M.: Asymmetry of SPECT perfusion image patterns as a diagnostic feature for Alzheimer's disease. *Med. Image Comput. Assist. Interv. Int. Conf.* 2006, 9(Pt 2), 421–428.
6. Olejarczyk E., Przytułska M.: Analysis of differences between SPECT images of the left and right cerebral hemispheres in patients with epileptic symptoms. *Biosignals 2008 International Conference on Bio-inspired Systems and Signal Processing*, 28–31 January 2008, Funchal, Madeira – Portugal.
7. Pruszyński B.: *Radiology. Image diagnostics RTG, TK, USG, MR and radioisotopes* (in Polish), PZWL, Warszawa 2006.
8. Russ J.C.: *Image processing handbook*. 2<sup>nd</sup> edition. CRC Press, Boca Raton, Ann Arbor, London 1995.
9. Shannon C.E.: A Mathematical Theory of communication. *The Bell System Technical Journal*, 1948, 27, 379–423, 623–659.
10. Kuczyński K., Mikołajczyk P.: Adjustment and segmentation of medical images based on elements of information theory (in Polish). *XIII Krajowa Konferencja Naukowa Biocybernetyka i Inżynieria Biomedyczna*, Gdańsk, 2003, 806–811.
11. Chen C., Daponte J., Fox M.: Fractal feature analysis and classification in medical imaging. *IEEE Trans. Med. Imaging*, 1989, 8, 133–142.
12. Oczeretko E.S.: *Fractal dimension in biomedical signal and image analysis* (in Polish), Wydawnictwo Uniwersytetu w Białymstoku, Białystok 2006.
13. Kuikka J.T. et al.: Imaging the structure of the striatum: a fractal approach to SPECT image interpretation. *Physiol. Meas.*, 19, 1998, 367–374.